Insect Biochemistry and Molecular Biology 109 (2019) 106–115

Contents lists available at ScienceDirect

Insect Biochemistry and Molecular Biology

journal homepage: www.elsevier.com/locate/ibmb

Characterization of the novel role of NinaB orthologs from *Bombyx mori* and *Tribolium castaneum*

Chunli Chai[a], Xin Xu[a], Weizhong Sun[b], Fang Zhang[a], Chuan Ye[a], Guangshu Ding[a], Jiantao Li[a], Guoxuan Zhong[a,c], Wei Xiao[d], Binbin Liu[e], Johannes von Lintig[f], Cheng Lu[a,*]

[a] State Key Laboratory of Silkworm Genome Biology, Key Laboratory of Sericultural Biology and Genetic Breeding, Ministry of Agriculture and Rural Affairs, College of Biotechnology, Southwest University, Chongqing 400715, China
[b] College of Animal Science and Technology, Southwest University, Chongqing 400715, China
[c] Life Sciences Institute and the Innovation Center for Cell Signaling Network, Zhejiang University, Hangzhou 310058, China
[d] College of Plant Protection, Southwest University, Chongqing 400715, China
[e] Sericulture Research Institute, Sichuan Academy of Agricultural Science, Chengdu 610066, China
[f] Department of Pharmacology, Case Western Reserve University, School of Medicine, Cleveland, OH 44106, USA

A B S T R A C T

Carotenoids can be enzymatically converted to apocarotenoids by carotenoid cleavage dioxygenases. Insect genomes encode only one member of this ancestral enzyme family. We cloned and characterized the *ninaB* genes from the silk worm (*Bombyx mori*) and the flour beetle (*Tribolium castaneum*). We expressed BmNinaB and TcNinaB in *E. coli* and analyzed their biochemical properties. Both enzymes catalyzed a conversion of carotenoids into *cis*-retinoids. The enzymes catalyzed a combined *trans* to *cis* isomerization at the C11, C12 double bond and oxidative cleavage reaction at the C15, C15′ bond of the carotenoid carbon backbone. Analyses of the spatial and temporal expression patterns revealed that *ninaB* genes were differentially expressed during the beetle and moth life cycles with high expression in reproductive organs. In *Bombyx mori, ninaB* was almost exclusively expressed in female reproductive organs of the pupa and adult. In *Tribolium castaneum*, low expression was found in reproductive organs of females but high expressions in male reproductive organs of the pupa and imagoes. We performed RNAi experiments to characterize the role of NinaB in insect reproduction. We observed that RNAi treatment significantly decreased the expression levels of *BmninaB* and *TcninaB* and reduced the egg laying capacity of both insects. Together, our study revealed that NinaB's unique enzymatic properties are well conserved among insects and implicate NinaB function in insect reproduction.

1. Introduction

In animals, carotenoids play critical roles as ornaments, blue light filters, and antioxidants (Demmig-Adams and Adams, 2002; Krinsky, 1993; Krinsky et al., 2003; Toews et al., 2017). These pigments also can be enzymatically converted to apocarotenoids, including retinoids, which serve as signaling molecules and chromophores in various physiological processes (von Lintig, 2010; von Lintig, 2012; Ziouzenkova and Plutzky, 2008).

In insects, the color of caterpillar integument, wings of butterflies, and cocoons of silkworm are related to the accumulation of carotenoids. Butterflies use these pigments as ornaments for warning, photo-protection, mate attraction, and concealment (Bybee et al., 2012; Mallet and Joron, 1999). For instance, the carotenoids lutein, β-carotene, cyptoxanthin and canthaxanthin were detected in the swallowtail *Battus philenor* adult (Rothschild et al., 1986). Phytoene, lutein, neoxanthin and flavoxanthin were identified in the common blue butterfly, *Polyommatus icarus* Rott (Feltwell and Valadon, 1970). Similarly, the colors of the silkworm cocoons derive from the specific accumulation of dietary carotenoids. Lutein and β-carotene are the major pigments which contribute to the yellow and red colors of the silk (Tsuchida and Sakudoh, 2015). In insect integument and hemolymph, carotenoids can be bound to proteins to give green, blue-green, blue and red colors (Grayson et al., 2008). Additionally, all insects convert carotenoids to retinoids (vitamin A and its derivatives) which are critical for insect vision (Harris et al., 1977; von Lintig et al., 2001).

In recent years, much progress has been made in identifying key players for carotenoid metabolism in insects. In *Drosophila*, carotenoids absorption and cellular uptake has been shown to be mediated by scavenger receptor NinaD and its related protein SANTA MARIA (Kiefer et al., 2002; Wang et al., 2007). The carotenoid cleavage dioxygenase and isomerase NinaB metabolize the carotenoids to the visual chromophore (Oberhauser et al., 2008; von Lintig and Vogt, 2000; Wang et al., 2007). In silkworm *Bombyx mori*, CBP, Cameo2 and SCRB15 are the key regulators selective absorption of carotenoids from dietary mulberries to specific tissues (Sakudoh et al., 2007, 2010, 2013).

* Corresponding author.
E-mail address: lucheng@swu.edu.cn (C. Lu).

https://doi.org/10.1016/j.ibmb.2019.03.004
Received 16 May 2018; Received in revised form 29 December 2018; Accepted 6 March 2019
Available online 11 March 2019
0965-1748/

The analysis of the *ninaB* mutant demonstrated that carotenoids are critical for *Drosophila* vision (Voolstra et al., 2010). However, the role of ninaB gene in other insect species has not yet been studied. We here cloned *ninaB* homologous gene from *Bombyx mori* and *Tribolium castaneum*. We expressed these genes in *E. coli* and characterized the biochemical properties of the recombinant proteins. We then screened select tissues for *ninaB* expression and found differential expression in reproductive organs of male and female of pupa/adult in both silkworm and red flour beetle. RNAi treatment caused a decrease in *ninaB* mRNA levels and resulted in a reduction of the number of eggs and additional abnormal phenotypes in the beetle. Thus, our study unravels a novel function of NinaB and implicates carotenoids in insect reproduction.

2. Materials and methods

2.1. Strains and culture of silkworm and beetle

The Silkworm strain Dazao was maintained at the Southwest University of China. Silkworms were reared on fresh mulberry leaves at 25 °C under a natural light/dark cycle. The Georgia-1(GA1) strain of *T. castaneum* was reared on whole-wheat flour containing 5% (w/v) of brewers' yeast in a 30 °C growth chamber with 65% humidity on a dark condition (Haliscak and Beeman, 1983; Parthasarathy et al., 2009). Pupae were separated by sex based on the genital papillae differences. The adult beetles with untanned cuticle which emerged soon were designated as 0 hand staged thereafter.

2.2. RNA extraction and reverse transcription polymerase chain reaction (RT-PCR)

RNA was isolated from a wide range of developmental stages and tissues of silkworm and beetles. For silkworm, we isolated RNA from silkworm embryo, larva, pupa and moth stages as well as different tissues of day 3 of the 5th instar larva (midgut, anterior silkgland, middle silkgland, posterior silkgland, integument, fat body, malpighian tubes, gonads, head and hemolymph). Beetles were collected at different developmental stages including embryo, larvae, pupa, adults. Larvae tissues (fat body, Malpighian tubes, midgut, hindgut, head, cuticle, ovary, testis, CNS) were dissected, RNA was isolated from whole animals and tissues using TRIzol® reagent (Invitrogen) according to the manufacture's protocol. Reverse transcription of RNA to cDNA was performed using oligo(dT) primer and M-MLV reverse transcriptase (Promega) according to the manufacture's protocol.

RT-PCR were performed using primer sets listed in Table 1. For *BmninaB*, the following RT-PCR conditions were employed: initial denaturation at 95 °C for 3 min, then 30 cycles of 95 °C for 30s, 60 °C for 30s and 72 °C for 90s. The cycling protocol was followed by a final extension step at 72 °C for 10min. The *rpl3* gene and *16S* gene were used as normalization control in *B. mori* and *T. castaneum*, respectively. For *TcninaB*, we used the following RT-PCR conditions: initial denaturation at 94 °C for 4 min, then 30 cycles of 94 °C for 30s, 60 °C for 30s and 72 °C 30s, followed by a final extension step at 72 °C for 10min.

2.3. High-performance liquid chromatography (HPLC) analysis of NinaB enzyme activity and products

HPLC analyses were carried out with an Agilent 1260 Infinity Quaternary HPLC system (Santa Clara, CA, USA) equipped with a pump (G1312C) with an integrated degasser (G1322A), a thermostatic column compartment (G1316A), an autosampler (G1329B), a diode-array detector (G1315D), and online analysis software (Chemstation). Analyses were performed at 25 °C using a normal-phase Zorbax Sil (5 μm, 4.6 × 150 mm) column (Agilent Technologies, Santa Clara, CA) protected with a guard column. Detection of carotenoids and retinoids was performed at 360 nm −430nm wavelength.

Enzymatic assays were carried out as previously described (Babino et al., 2016). OTG micelles loaded with substrate were prepared as follows: 33 μL 10% OTG detergent solution was mixed with 2000 pmol (final concentration 20 μM) of substrate, dissolved in acetone, in a 2-mL Eppendorf tube. This mixture was then dried in a Speedvac (Eppendorf Vacufuge Plus). To substrate, 100 μL of cell lysate was added and vortexed vigorously for 20 s and then placed on an Eppendorf thermoshaker set at 28 °C for 8 min at 300 rpm. Control assays were performed with non-induced *E. coli* cell pellet lysates. Reactions were stopped by adding 100 μL of water and 400 μL of acetone. Lipids were extracted by adding 400 μL of diethyl ether and 100 μL petroleum ether, then vortexed for 3 × 10 s periods, centrifuged at 15,000 × *g* for 1 min and finally the resulting organic phase was collected. The extraction was performed twice and the collected organic phase was dried in a Speedvac. The dried supernatant then was re-dissolved in mobile phase (90:10 (v/v) hexane: ethyl acetate for β, β-carotene and 70:30 (v/v) hexane: ethyl acetate for zeaxanthin) and subjected to HPLC analysis. The flow rate for all systems was 1.4 mL/min.

Table 1
Primers used to amplify *BmninaB and TcninaB* genes. Lowercase letters in the primers for dsRNA synthesis are T7 polymerase promoter sequences.

Primers name		Sequence (5′-3′)
For cloning	*TcninaB*-F	AACGATGGCATCACAGAG
	TcninaB-R	CTTGACGTTTCTCCCAAT
	BmninaB-F	AGATTTTTAGTTACAATGGCTGC
	BmninaB-R	AATATTAGTAGTTTGTGGGAGAAAC
For RT-PCR and qPCR	TcninaB -QF	CCAGAATCAACTATGGGCAA
	TcninaB-QR	GTGTCTTCTCTACCCCAT
	Tc16S—F	TTCGCCTGAATACTGTGTGC
	Tc16S-R	CTGATCGCTTTCGAACCTCT
	BmninaB-rtF	GCGATTCGAGTGTTTGGTTGAGAT
	BmninaB-rtR	TAAGCAGGAAAGACGGCAAGGAGT
	Rpl3-F	TTCCCGAAAGACGACCCTAG
	Rpl3-R	GAAACCTCCCATCGGTGTAAT
	BmninaB-QF	CTAAGCAGGAAAGACGGCAAGG
	BmninaB-QR	GTCAGCGTTACTTTGCATAGTCTCGA
For dsRNA synthesis	ds*TcninaB*-F	taatacgactcactatagg GTTGCCTTCTACGTAATGGAC
	ds*TcninaB*-R	taatacgactcactatagg CTGAGTAAAATTTGTAAGCCAG
	ds*BmninaB*-F	taatacgactcactatagg GCGATTCGAGTGTTTGGTTGAGAT
	ds*BmninaB*-R	taatacgactcactatagg TAAGCAGGAAAGACGGCAAGGAGT

2.4. RNA interference

We used primers tailed with T7 promoters on the 5′ side to synthesize gene-specific dsRNA, which target the RPE65 domain sequences. RNAi was carried out to evaluate the role of *BmninaB* and *TcninaB* in development. dsRNAs were synthesized using RiboMAX™ Large scale RNA production system-T7 Kit (Promega) according to manufacturer's manual. The primers used for dsRNA synthesis are listed in Table 1. The diagrammatic position and sequences for those RNAi targeted are shown in Supplemental Fig. 1 and Supplemental Fig. 2. For *Bombyx mori*, we injected 150 μg *BmninaB* dsRNA per pupa at the stage of 4d after cocooning. The weight of Dazao pupa is about 700–1000 mg which is almost 250 times of beetle 20d larva's weight. The late (20-day) beetle larvae were selected for injections of *TcninaB* dsRNA (ds*TcninaB*) at doses 800 ng/larva. The mortality owing to injection damage was smaller than 10%. The injected insects were reared under standard conditions and phenotypes were recorded every day after the injection. qPCR was used to monitor the change of the *TcninaB* expression after the injection of dsRNA.

To examine effects of ds*TcninaB* injection on insect growth and development, a large number of 20-day larvae were injected with ds*TcninaB* or buffer as controls. After the injected larvae developed into pupae, we gathered statistics from pupation rate and the following

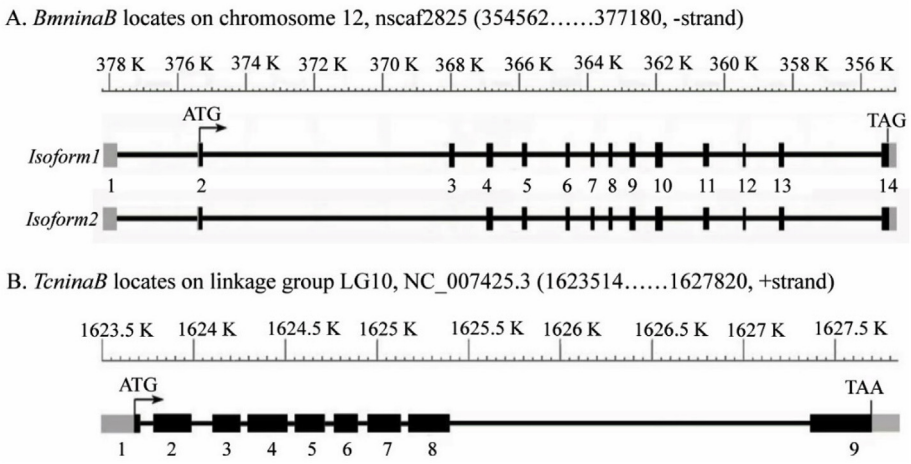

Fig. 1. Structure of *BmninaB* and *TcninaB* genes.

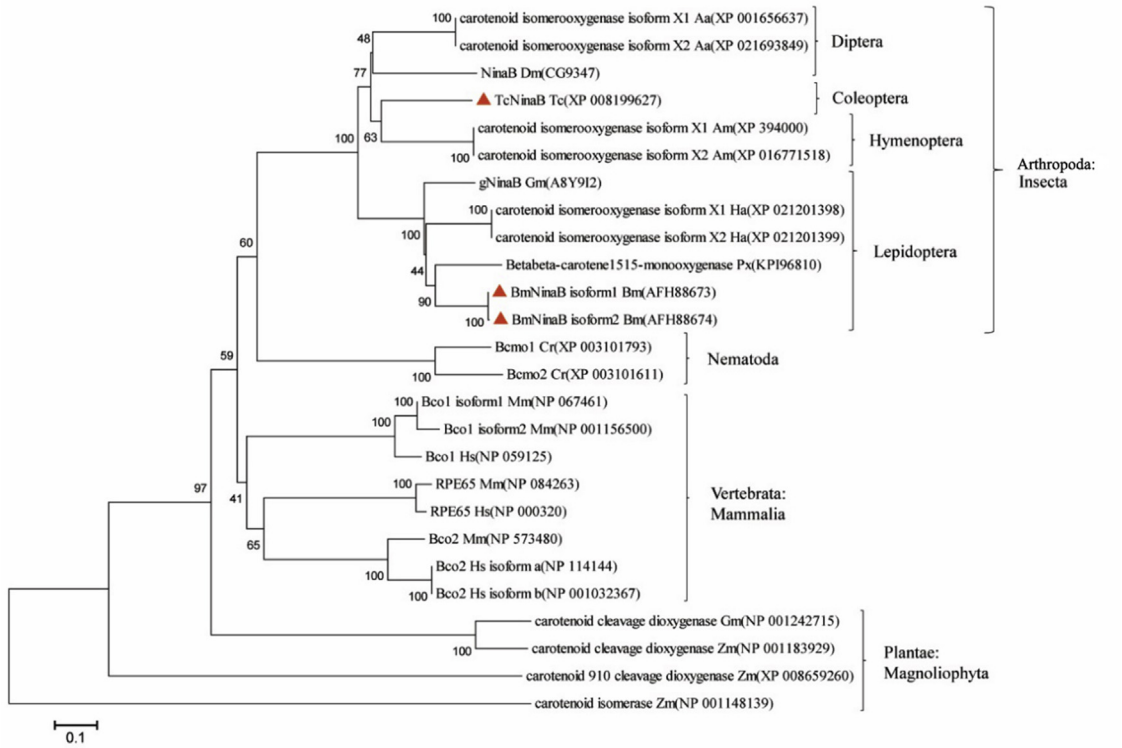

Fig. 2. Phylogenetic analysis of NinaB orthologs from different species. The evolutionary history was inferred using the Neighbor-Joining method. Accession numbers are shown in brackets after taxa names. The percentages of bootstrap values are shown next to branches. The triangles are shown before TcNinaB and BmNinaB. Abbreviations: Aa, *Aedes aegypti*; Dm, *Drosophila melanogaster*; Tc, *Tribolium castaneum*; Am, *Apis mellifera*; Gm, *Galleria mellonella*; Ha, *Helicoverpa armigera*; Px, *Papilio xuthus*; Bm, *Bombyx mori*; Cr, *Caenorhabditis remanei*; Mm, *Mus musculus*; Hs, *Homo sapiens*; Gm, *Glycine max*; Zm, *Zea mays*.

eclosion rate, meanwhile separating the males and females at 5-day pupae. At 5 days post-eclosion, we paired the same period adults as follows: 1) male and female adults from wild type larvae; 2) male and female adults raised from larvae injected with buffer; 3) male and female adults from the larvae injected with ds*TcninaB*. Each treatment group consisted of at least eight mating pairs, and each experiment was repeated three times with at least 30 individuals. Beetle eggs were collected after mating five days, whereas egg hatchability was examined five days after the eggs were collected. After mating, we carefully observed the beetles' phenotypic appearance and the remaining dorsal body fat content. We also dissected the mated adults to examine whether testis displayed abnormal phenotypes as compared with controls. In addition, we weighed adults individuals from 3- and 5- days post-eclosion, and 5 days after mating following the injections of ds*TcninaB*.

2.5. RT-qPCR

The relative transcript levels of *BmninaB* and *TcninaB* were analyzed by qPCR using SYBR Green with the StepOne real-time PCR detection system. qPCR was performed with three biological replicates, each with two technical replicates. The transcript levels of *TcninaB* were expressed as normalized transcript abundance using *Tc16s* as an internal reference gene. The relative *TcninaB* transcript levels were calculated with the $2-\Delta\Delta Ct$ method.

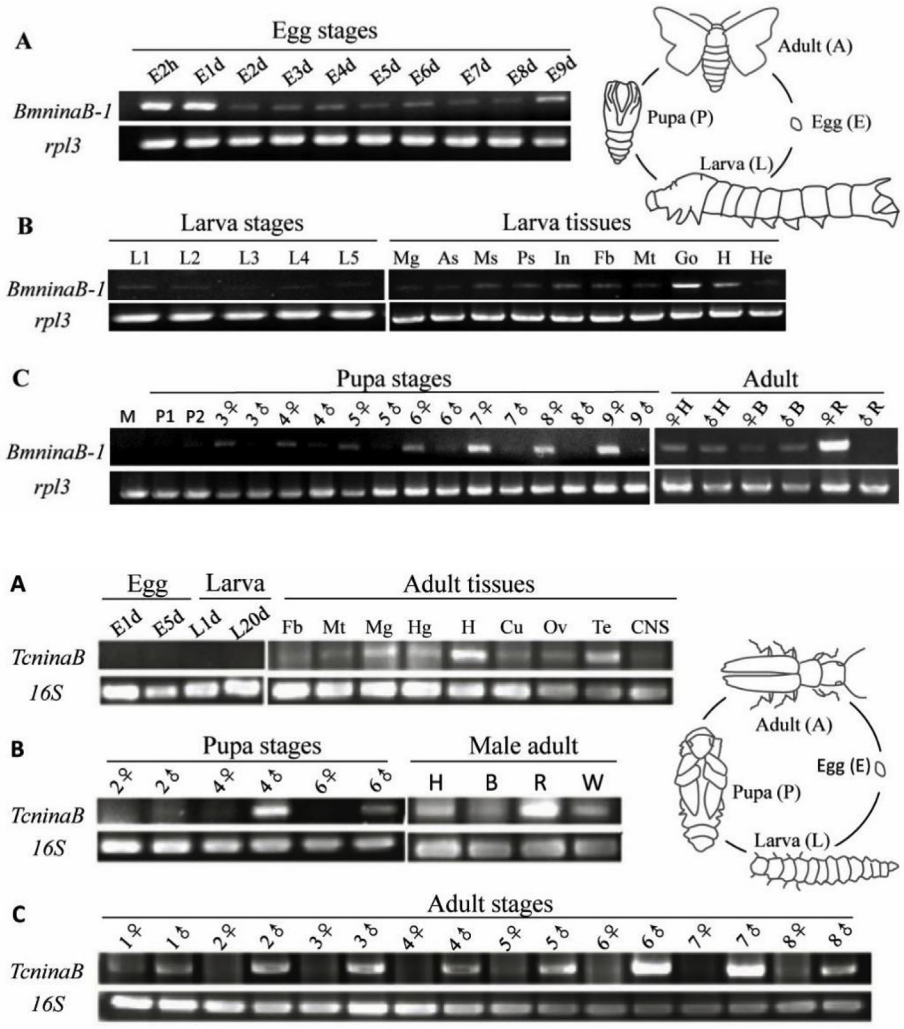

Fig. 3. Expression patterns of *BmninaB* in different tissues and different developmental stages. (A) E2h, 2 h after egg laying(AEL); E1d, 1d AEL; E2d, 2d AEL; E3d, 3d AEL; E4d, 4d AEL; E5d, 5d AEL; E6d, 6d AEL; E7d, 7d AEL; E8d, 8d AEL; E9d, 9d AEL. (B) L1-L5 is new molted silkworm for 1st instar, 2nd instar, 3rd instar, 4th instar and 5th instar, respectively. Tissue samples is from 3rd day of 5th instar larva. Mg, midgut; As, anterior silkgland; Ms, middle silkgland; Ps, posterior silkgland; In, integument; Fb, fat body; Mt, Malpighian tubes; Go, gonads; H, head; He, hemolymph. (C) M, gonads from mature silkworm; P1 and P2, mixed ovaries and testis from 1d to 2d pupa, respectively. 3♀, 3♂ −9♀, 9♂ are reproductive system samples from pupa of 3d, 4d, 5d, 6d, 7d, 8d and 9d, respectively; ♀H, head of female moth; ♂H, head of male moth; ♀B and ♂B are samples from female and male moth body parts (after deletion of head and reproductive systems), respectively. ♀R and ♂R are reproduction systems from female moth and male moth, respectively.

Fig. 4. Expression patterns of *TcninaB* in different tissues and different developmental stages. (A) E1d, 1d embryo; E5d, 5d embryo; L1d, 1d larva; L20d, 20d larva; Fb, fat body; Mt, Malpighian tubes; Mg, midgut; Hg, hindgut; H, head; Cu, cuticle; Ov, ovary; Te, testis; CNS, central neuron system. (B) 2♀, 2♂ −6♀, 6♂ are ovary samples from 2d, 4d and 6d female pupas and male pupas. H, head of male beetle; B, body remainder (except head and testis) of male beetle; R, male reproductive of male beetle; W, the whole body of male beetle; (C) 1♀, 1♂ −8♀, 8♂ are reproductive system samples from female and male beetles of 1d, 2d, 3d, 4d, 5d, 6d, 7d and 8d, respectively.

2.6. Site-directed mutagenesis

Mutagenesis of BmNinaB was performed using the QuikChange XL site-directed mutagenesis kit (Agilent). Mutants were firstly verified by sequence analysis of plasmids purified by QIA quick purification kits (Qiagen). The primers used were H312A: 5′-CAAAGCAGTTGATGATG GCAAGGAAGAAGAGGGTCT-3′ and 5′- GACCCTCTTCTTCCTTGCCATC ATCAACTGCTTTG-3'; E387S: 5′- GTATCCTCGGAGTCGAACAGCCGAG GTCGG-3′ and 5′- CCGACCTCGGCTGTTCGACTCCGAGGATAC-3'. The sequencing-verified mutated plasmids were transformed into β-carotene producing XL1Blue competent cells. The bacteria pellets were collected, lysis, the lipid crude extracts were undergone HPLC analysis.

3. Results

3.1. Cloning of BmninaB and TcninaB

We identified a *Drosophila ninaB* orthologous gene in the silkworm genome. *BmninaB* (Accession no. AFH88673) is located on the reverse strand of nscaf2825 on chromosome 12. The gene consists of 14 exons and encoded two mRNA isoforms, isoform1 and isoform 2. The length of isoform1 is 2139bp, encoding a 511-amino acid long putative protein. The length for 5′UTR is 381bp and the length of the 3′ UTR is 222bp. The total length of isoform2 mRNA transcript is 2028bp. This putative splicing variant lacks exon3 of isoform 1 and encodes for 474 amino acids long putative protein (Fig. 1A). Both transcripts are predicted to encode a protein containing the RPE65 domain which is characteristic for this protein family. The BmNinaB protein shares 78% sequence identity with *Amyelois transitella*, 54% with *T. castaneum*, 55% with *Drosophila* NinaB, and 34% with human RPE65, respectively.

In the *T. castaneum* genome, we also identified a *TcninaB* orthologous gene based on sequence identity to other insect *ninaB* genes. The gene is located on Nc_007425 of linkage group 10. The predicted mRNA sequence was completely identical to the sequence published in NCBI (accession no. XM_008201405). Our analysis showed that *TcninaB* gene consisted of 9 exons and that the length of its predicted mRNA was 1919bp and encoded for 531 amino acids (Fig. 1B). The TcNinaB shared the highest sequence identity of 68% with *Aethina tumida*. It shared 57% identity with *Drosophila* NinaB and 35% identity with human RPE65, respectively.

Carotenoid cleavage dioxygenases were identified from a diverse set of species. The phylogenetic analysis on these enzymes reveals that BmNinaB was firstly grouped with Lepidopteran orthologs, including *H. armigera*, *G. mellonella* and *P. xuthus*, then grouped with orthologs from other insects. All the mammalian NinaB homologs grouped together in the phylogenetic dendrogram. Vertebrate Bco1, Bco2 and RPE65 grouped in different branches which indicated these genes evolved independently before the separation from insect homologs (Fig. 2).

3.2. Spatial and temporal expression profiles of BmninaB and TcninaB

Gene expression patterns of *BmninaB* and *TcninaB* were analyzed by reverse transcriptase-polymerase chain reaction (RT-PCR) in different developmental stages of *B. mori* and *T. castaneum* and different tissues

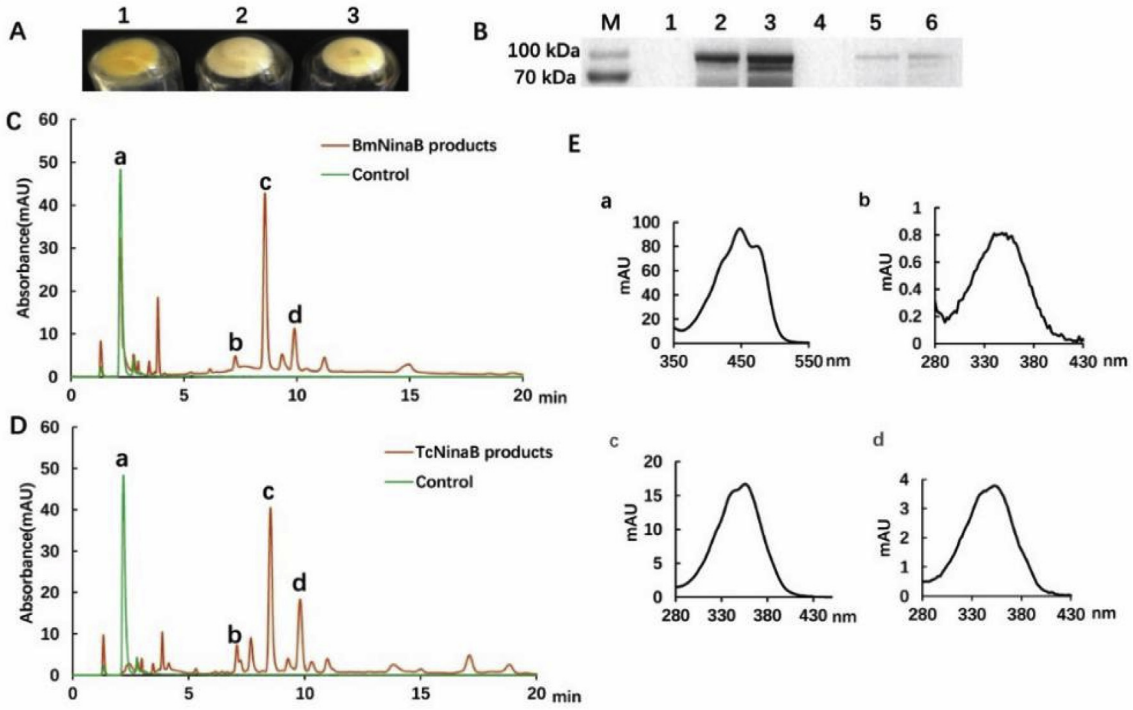

Fig. 5. Enzymatic activity tests with BmNinaB and TcNinaB. (A) Comparison on the pellets' color before and after cleavage of β-carotene to retinoids in *E. coli*. 1. pellet from β-carotene producing *E. coli* only. 2. pellet from β-carotene producing and BmNinaB expressed *E. coli.* 3. pellet from β-carotene producing and TcNinaB expressed *E. coli.* 4, 5 and 6 were the upper layer of the samples from 1, 2, and 3, respectively. (B) Western blotting detection on the expression of *BmninaB* and *TcninaB* in *E. coli*. (C) & (D) HPLC profiles at 350 nm of lipid extract from an *in vitro* test for BmNinaB and TcNinaB enzymatic activity, respectively. a, β, β-carotene; b, 11-*cis*-retinaloxim(syn); c, all-*trans*-retinaloxim(syn); d, 9-*cis*-retinaloxim(syn); (E) UV/vis spectra of corresponding peaks a, b, c and d in (C) & (D). (For interpretation of the references to color in this figure legend, the reader is referred to the Web version of this article.)

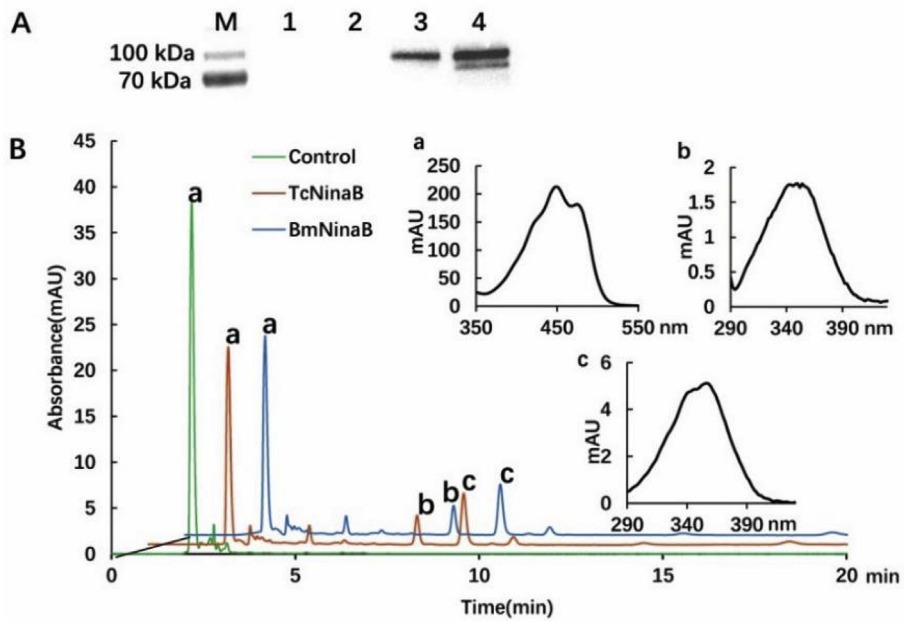

Fig. 6. Tests for enzyme activity of BmNinaB and TcNinaB on β, β-carotene. (A) Western blotting detection on the expression of recombinant *BmninaB* and *TcninaB* in XL1blue bacteria, respectively. 1 and 3 were pellet samples of BmNinaB recombinant protein before and after IPTG induction, respectively; 2 and 4 were pellet samples of TcNinaB recombinant protein before and after IPTG induction, respectively. (B) HPLC profiles at 360 nm of lipid crude extracts from *in vitro* tests for enzyme activity using BmNinaB and TcNinaB cell lysate and β, β-carotene as a substrate. a, b and c are the UV/vis spectra of corresponding peaks in (B). a, β, β-carotene; b, 11-*cis*-retinaloxim(syn); c, all-*trans*-retinaloxim(syn).

of larvae. *BmninaB* showed high mRNA expression levels in unfertilized eggs and eggs one day after egg laying. Later, NinaB was continuously expressed in low level until hatching (Fig. 3A). We also detected low expression of *BmninaB* in freshly molted silkworm of each larvae instar. In tissues of 3d 5th instar silkworm larvae, *BmninaB* was strongly expressed in gonads and the head. It also was expressed at low levels in other tissues (Fig. 3B). Interestingly, we observed high *BmninaB* expression in female reproductive systems of pupa and moth whereas *BmninaB* expression was absent or low in the male reproductive system. The expression of *BmninaB* seemed to increase during silkworm pupa maturation. We further examined the expression of *BmninaB* in different body parts of male and female moth and observed major differences between female and male reproductive systems but not in others tissues (Fig. 3C).

In embryonic and larvae stage of *Tribolium*, we did not detect any expression of *TcninaB*. The expression of *TcninaB* was firstly detected in

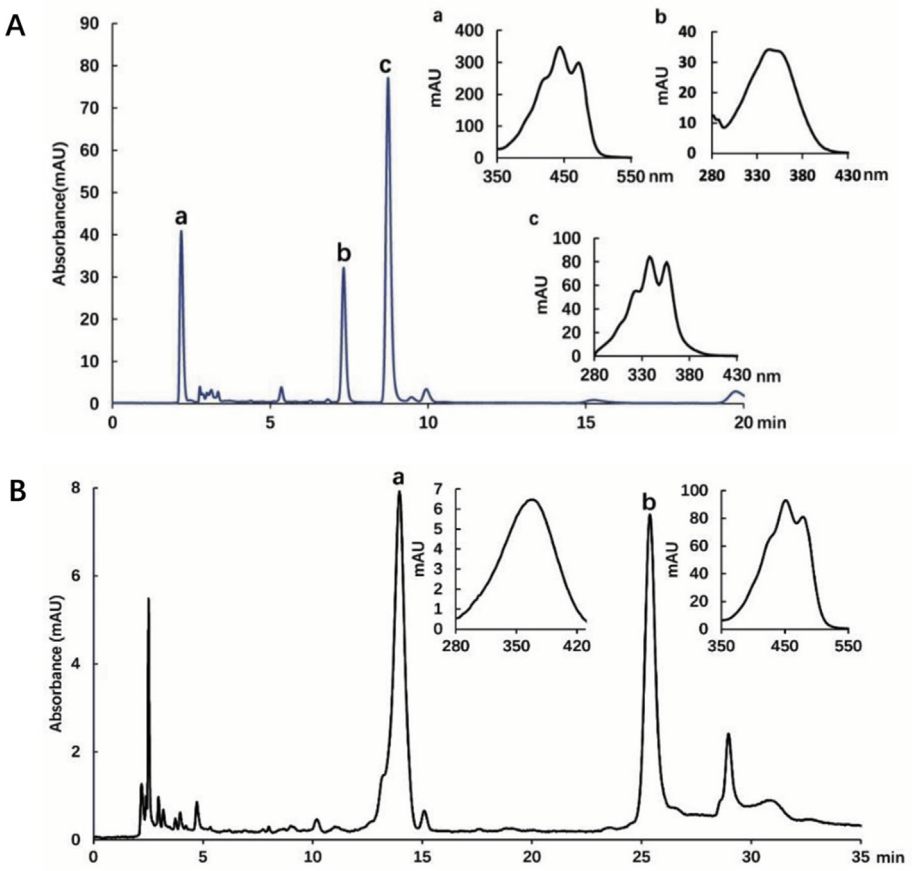

Fig. 7. Test for enzyme activity of BmNinaB on α-carotene (A) and zeaxanthin (B). In Fig. 7A, a, α-carotene; b, 11-*cis*-retinaloxim (syn, with β-ionone ring); c, *trans*-α-retinaloxim (syn, with ε-ionone ring). In Fig. 7B, a, 11-*cis*-retinaloxim; b, zeaxanthin. The UV/vis spectra of corresponding peaks are shown in the figure.

pupa stage and *TcninaB* showed apparently high expression levels in males when compared to females (Fig. 4B). Further examinations revealed that *TcninaB* was differentially and high expressed in the male reproductive systems of adult beetles while only faint amplification bands were obtained from RNA samples of female reproductive organs (Fig. 4C). In the male beetle, we detected that *TcninaB* was highly expressed in the reproductive system compared with other body parts. Regarding tissue distribution, *TcninaB* was moderately expressed in head, testis, and midgut. Low expression was found in other tissues with our RT-PCR protocol (Fig. 4A).

3.3. BmNinaB and TcNinaB polypeptide catalyze oxidative cleavage and isomerization

In order to study the enzymatic function of BmNinaB and TcNinaB, both genes were expressed as GST-tagged protein in *Escherichia coli* (*E. coli*). We transformed recombinant *BmninaB* and *TcninaB* plasmids into β-carotene producing *E. coli* (XL1Blue). This strain contains another plasmid with the gene set of β-carotene biosynthesis. Upon overnight growth, we found a color shifts from yellow to almost white in *E. coli* expressing the insect NinaBs when compared to *E. coli* controls transformed with the vector alone (Fig. 5A). We confirmed the expressions of the recombinant insect NinaB fusion proteins by Western blotting using antibodies directed against the GST tag of the recombinant protein (Fig. 5B). Additionally, we extracted lipids from the *E. coli* strains and subjected them to HPLC analysis. Results from HPLC also showed both BmNinaB and TcNinaB had high enzymatic activities to cleavage the β-carotene product into retinoids, including all-*trans*-retinal and 11-*cis*-retinal (Fig. 5C and D).

We next performed tests for enzymatic activities with recombinant BmNinaB and TcNinaB protein extracts in the presence of 3% octyl β-D-1-thioglucopyranoside (OTG) and 16 μM β, β-carotene. Enzyme assays were stopped after 12 min and lipids were extracted and subjected to HPLC analysis. Results showed that both BmNinaB and TcNinaB were bifunctional and catalyzed an oxidative cleavage reaction at C15, C15' and a *trans*-to-*cis* isomerization reaction at C11, C12. With symmetric β, β-carotene substrate this reaction resulted in the formation of one molecule 11-*cis*-retinal and one molecule all-*trans*-retinal (Fig. 6). We previously showed that the *trans*-to-*cis* isomerization reaction preferentially occurred at C11, C12 adjacent to a β-ionone ring site of the carotenoid substrate(Babino et al., 2016). To test whether this ring site selectivity of NinaB is conserved between different insect species we incubated BmNinaB in the presence of α-carotene with one β- and one ε-ionone ring site. Analyses of the enzymatic reaction products by HPLC revealed that the asymmetric carotenoid was converted into 11-*cis*-retinal and all-trans-α-retinal, indicative for an isomerization at C11, C12 adjacent to the β-ionone ring site of the carotenoid substrate (Fig. 7A). We also performed test for enzymatic activity with zeaxanthin which contains two hydroxylated β-ionone ring sites. In fact, BmNinaB efficiently catalyzed the conversion of zeaxanthin to 3-hydroxy-retinoids (Fig. 7B). This indicated that xanthophylls which are major dietary carotenoids of *Bombyx* can be utilized for retinoid production.

We next tested whether the basic mechanism of enzyme catalysis is conserved in insects. It was reported that ferrous iron (Fe^{2+}) is indispensable for activating oxygen in cleavage of carotenoid/apocarotenoids substrates (Borowski et al., 2008). The ferrous iron is coordinated by four His residues and 3 s shell Glu residues which form a coordination sphere to keep the ferrous iron in the active center of these enzyme (Sui et al., 2013). Sequence alignments indicated that these

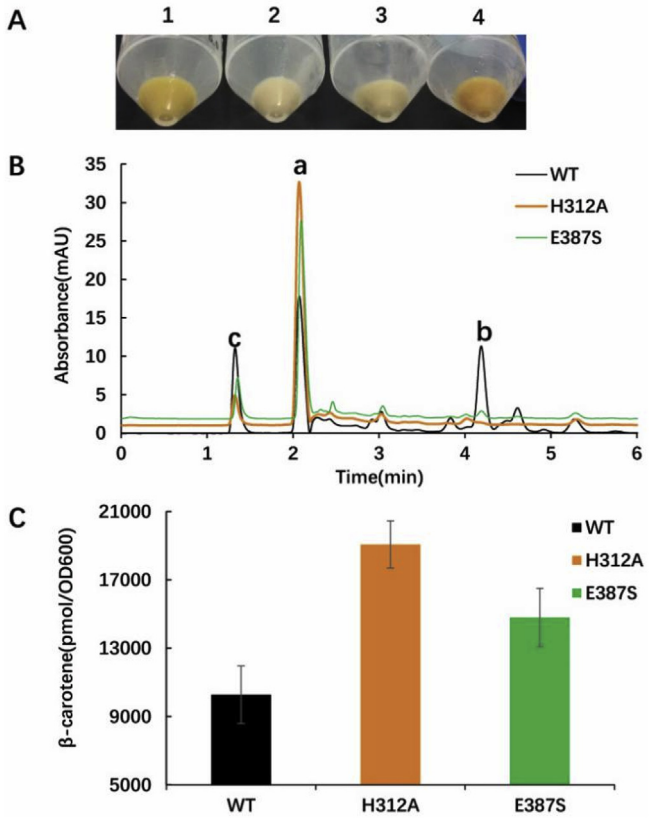

Fig. 8. Effects of site-directed mutagenesis on BmNinaB residues. (A) Comparison on the *E. coli* pellets' color between BmNinaB wildtype and BmNinaB mutants. 1, β-carotene producing XL1Blue bacteria; 2, BmNinaB wildtype expressed in β-carotene producing XL1Blue bacteria; 3, BmNinaB-G387S mutant expressed in the same bacteria; 4, BmNinaB-H312A mutant expressed in the same bacteria. (B) HPLC profiles at 350 nm of lipid extract from an *in vitro* test for BmNinaB wildtype and mutants' enzymatic activity. a, β-carotene; b, all-*trans*-retinaloxium(syn); c. bacterial metabolite. (C) Effects of site-directed mutagenesis on residues on BmNinaB catalytic activity measured by the production of β-carotene. (For interpretation of the references to color in this figure legend, the reader is referred to the Web version of this article.)

Table 2
BmninaB dsRNA interference in 4th day of silkworm cocooning stage.

Groups	Number of pupa for injection	Mortality	Number of moth for examination
BmninaB RNAi	30	0	29
ddH_2O control	30	0	26
WT	30	0	30

amino acids were well conserved in the insect enzymes (His184, His242, His312 and His501 in BmNinaB; His189, His245, His315, and His525 in TcNinaB). Thus, we performed site directed mutagenesis to introduce His312Ala and Glu387Ser mutation in to BmNinaB protein. We then expressed the recombinant proteins in the *E. coli* test system. The color of the bacterial cell pellets did not show the pronounced color shift from yellow to white though a slight color shift was still observed in the Glu387Ser mutant (Fig. 8A). HPLC analyses of lipid extracts revealed that the enzymatic activity was highly diminished in the cells expressing the His312Ala and Glu387Ser, respectively. There was no all-*trans* retinal produced by the mutant proteins when expressed in β-carotene producing XL1Blue cells (Fig. 8B). The amounts of β-carotene in cells expressing His312Ala mutant and Glu387Ser mutant proteins were almost twice times and 1.5 times of those expressing BmNinaB wildtype protein, respectively (Fig. 8C).

3.4. The decrease of BmninaB expression in pupa cause the reduction in egg-laying number of Bombyx mori

In order to verify the roles of *BmninaB* in the female reproductive system, we performed RNAi experiments of *BmninaB* in silkworm early pupa of the 4th day cocooning (Table 2). Results showed the expression of *BmninaB* decreased dramatically and that the decrease in expression did apparently not affect the survival of the silkworm pupa (Fig. 9A). Because *BmninaB* was highly expressed in the reproductive organ, we counted the number of eggs in each moth which developed from injected pupae. Our analyses revealed that the number of eggs in moth decreased 14% after *BmninaB* RNAi compared with the uninjected control (Fig. 9B). Further inspection indicated that the ovarian tubes were slightly shortened but the shortening was not statistically significant (Fig. 9C). We did not observed significant differences in the body weight of RNAi treated moths and controls. The behavior of moth ovulation after RNAi treatment also seems normal.

3.5. The decrease of TcninaB expression causes a reduction in reproductive capacity and abnormal phenotype in Tribolium castaneum

Since RNAi approaches in silkworm may not work as efficient as in Tribolum, we further conducted *TcninaB* RNAi experiments in Tribolum. After injection of 800 ng ds*TcninaB* RNA into 20-day beetle larva, we statistically analyzed the impact of the treatment on beetle development. Our analysis showed that the pupation rate and eclosion rate did not significantly differ between treatment groups (Fig. 10 A and Fig. 10B). However, the number of eggs decreased dramatically by 63.0% in the corresponding adults when compared with control which were injected with the same amount of PBS buffer (Fig. 10D). Notably, hatching rate of the remaining eggs did not show any significant differences between groups (Fig. 10C). In addition, we weighed the adult beetles at three stages (3- and 5- days post-eclosion, and 5 days after mating) after *TcninaB* dsRNA injection. We found that the weight of

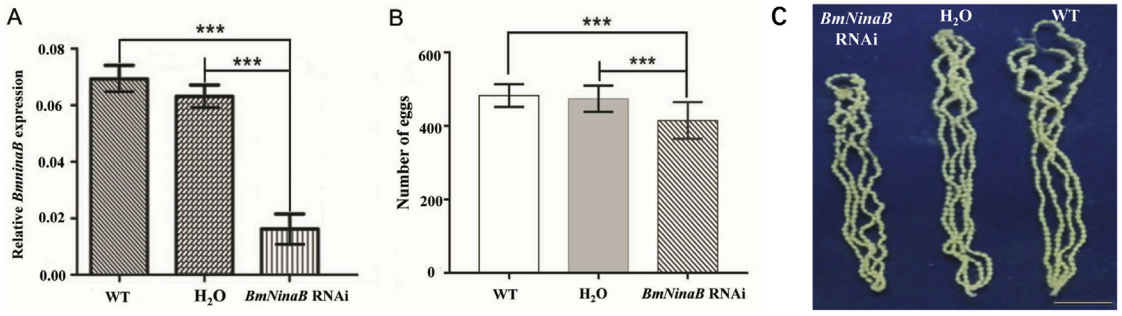

Fig. 9. Detection at the molecular level and egg number statistics after interference of *BmninaB*. (A) Real-time PCR detection at the molecular level after interference of *BmninaB*. (B) Egg number statistics after *ninaB* RNAi. (C) Comparison on the ovarian tubes of female mothes between *BmninaB* RNAi individuals and controls. The bar in Fig. 9c is 1 cm.

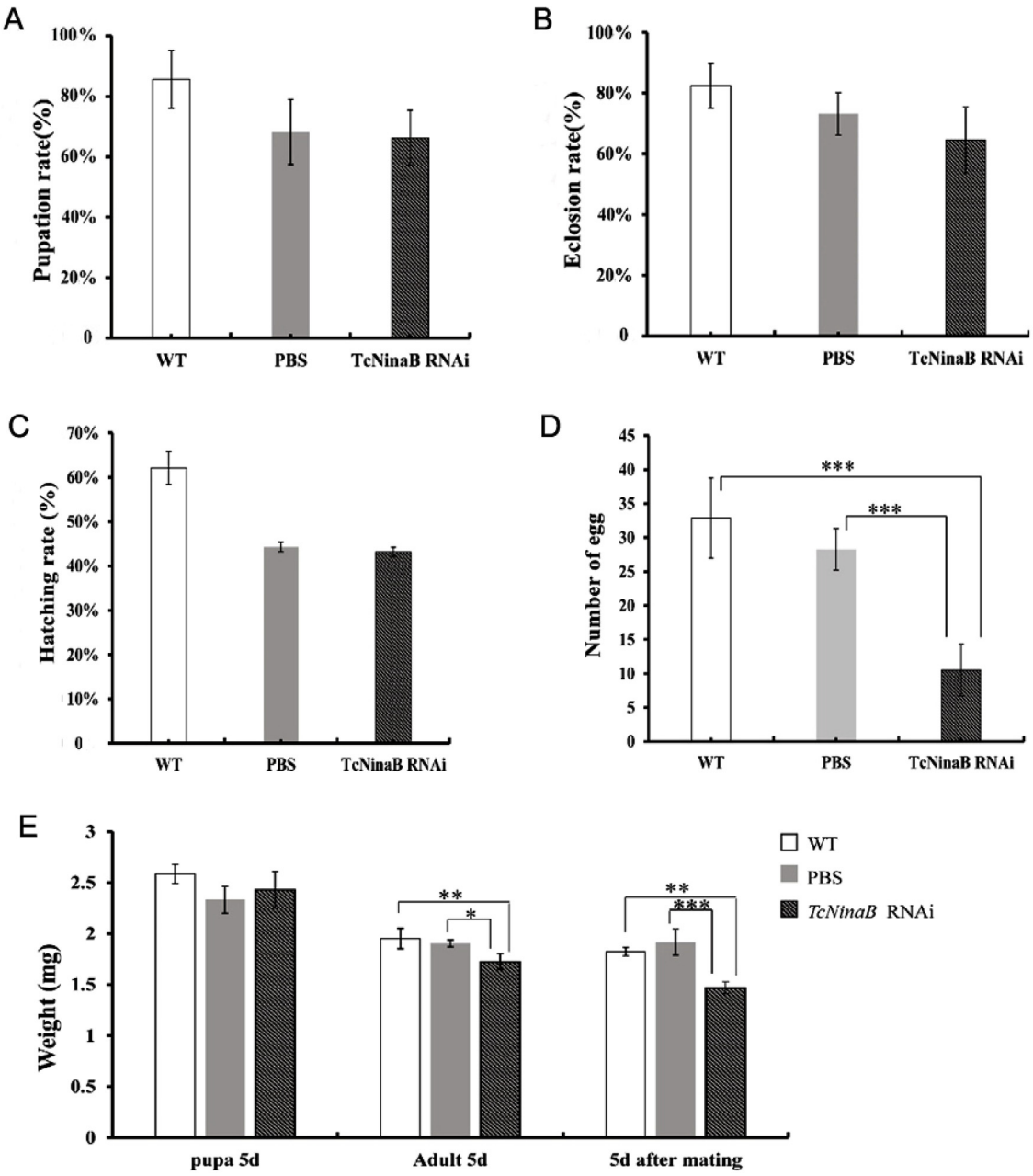

Fig. 10. The effect of *TcninaB* RNAi on the pupation(a), eclosion (b), egg hatching rate(c), number of eggs(d) and the weight of adults(e).

beetles with *TcninaB* dsRNA injection were lower by 9.4% and 23.3% compared with control adults 5- days post-eclosion and 5 days after mating, respectively (Fig. 10E).

We performed RT-qPCR to demonstrate that this phenotype was associated with a down regulation of the expression of TcNiniaB. The analysis demonstrated that *TcninaB* mRNA dramatically decreased, and that the effect lasted for a long time at least until 5 days after mating (Fig. 11A). The RNAi treatment caused approximately 73% of male reproductive systems with abnormal phenotypes of small size and light-colored testes (Fig. 11B). We also observed that 56.3% of male adults displayed abnormalities in membranous wings such as light color, and incompletely formed wings when compared with wild type beetles and buffer-injected beetles. When we removed the two pairs of wings, we also observed that about 51.8% ds*TcninaB*-treated adults exhibited a shriveled phenotype of the abdomen.

4. Discussion

Previous studies on the carotenoid cleavage oxygenase (CCO) in insects mainly focus on Drosophila vision. However, carotenoids and their retinoid metabolites have been implicated in additional physiological processes in insect biology. In the present study, we identified and biochemically characterized NinaB from *Bombyx mori* (*BmninaB*) and *Tribolium castaneum* (*TcninaB*). We studied their expression profiles throughout the life and performed loss of function analyses with dsRNA to unravel putative non-visual roles of the vitamin A forming enzyme in insects.

Bombyx mori (Lepidoptera), *Tribolium castaneum* (Coleoptera), and *Drosophila melanogaster* (Diptera) represents the three major clads of the genus Insecta. Our study showed that similar to *Drosophila* only a single member of carotenoid cleavage dioxygenase gene family exists in the genomes of *Bombyx* and *Tribolium*. Our biochemical studies with recombinant proteins demonstrated that BmNinaB and TcNinaB, similar

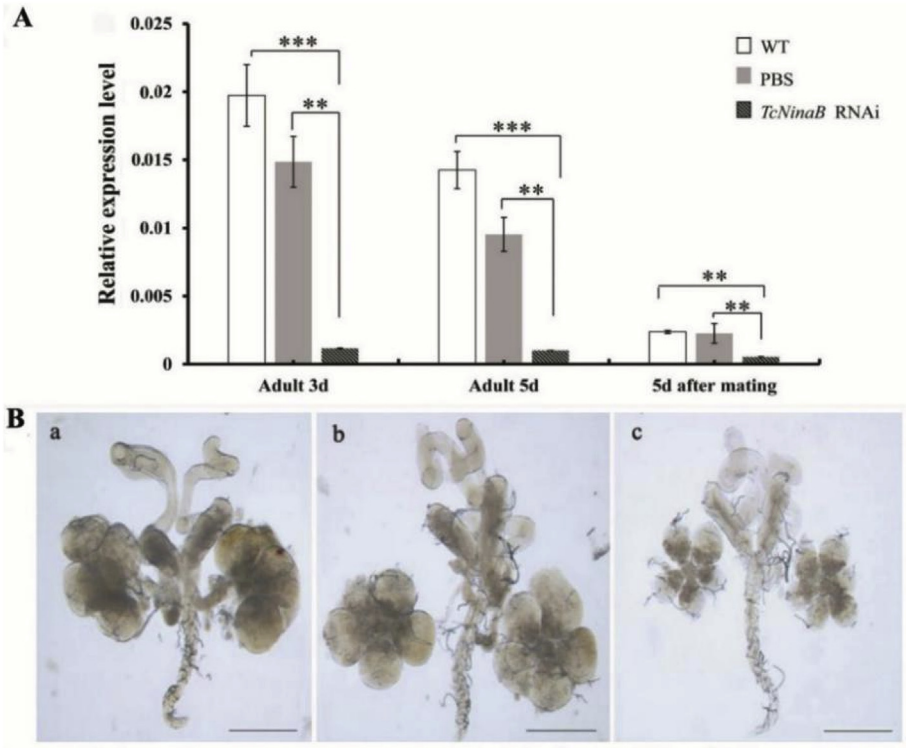

Fig. 11. Detection of *TcninaB* expression after ds*TcninaB* injection and effects of ds*TcninaB* injection on male reproductive system and external phenotypes. (A) Time-dependent suppression of *TcninaB* transcript in 20-day larvae of *T. castaneum* injected with ds*TcninaB* at 800 ng/larvae and isovolumetric PBS buffer, and compared with wild type at the same time determined by RT-qPCR. Different numbers of asterisks above the standard error bars indicate significant differences based on ANOVA followed by Fisher's LSD multiple comparisons (*$0.05 < P < 0.1$, **$0.01 < P < 0.05$, ***$P < 0.01$) within the same time point. (B) Effects of ds*TcninaB* injection on male reproductive system. (a)wild type, (b)PBS-treated, (c)injected with ds*TcninaB* at 800 ng/larvae.

to *Galleria* and *Drosophila* NinaBs, are multifunctional enzymes. These enzymes catalyzed the oxidative cleavage reaction at the C15, C15' double bond and concomitantly a *trans* to *cis* isomerization at the C11, C12 double bond of their carotenoid substrates. For enzyme catalysis, the ferrous iron in the active center plays a critical role (Sui et al., 2013). We provided evidence that the mechanism of catalysis is well conserved because site directed mutagenesis of iron coordinating amino acids rendered BmNinaB inactive. Additionally, we showed for BmNinaB and α-carotene that the enzyme displayed selectivity for the β-ionone ring of this asymmetric carotenoid substrate. Thus, the enzyme specifically converted this carotenoid into 11-*cis*-retinal and all-*trans*-α-retinal. 11-*cis*-retinal and 3-hydroxy-11-*cis*-retinal serve as the unique chromophores in insect vision (Isono et al., 1988; Seki and Vogt, 1998). The *cis*-configuration of the chromophore is essentially required for the maturation of the visual pigments during the development of the insect compound eyes (Oberhauser et al., 2008). In flies, genetic mutations in *ninaB* cause chromophore-deficiency and render mutants blind (von Lintig et al., 2001). Based on the conducted biochemical studies and the observed expression pattern of NinaB in the larval head of *Bombyx* and *Tribolium*, we conclude that the bipartite function as combined carotenoid oxygenase and isomerase of NinaB in chromophore production is well conserved among distantly related insect clades.

Surprisingly, our analyses also revealed that *BmninaB* and *TcninaB* are highly expressed in gonads and reproductive systems of pupa and adult. This contrast previous findings in *Drosophila* in which *ninaB* expression was found to be restricted to Bolwig's organ of the larva (Voolstra et al., 2010; Weiszmann et al., 2009), and the heads of the pupa and imagoes (Yang and O'Tousa, 2007). RNAi treatment decreased *ninaB* expression and was associated with the reduction in the number of eggs in *Bombyx* and *Tribolium* and morphological changes of the testes in Tribolium.

To our knowledge this is first experimental evidence that NinaB plays a significant role in reproduction of insects. A possible explanation might be that NinaB is required for chromophore production as needed in non-visual photo-perception. It was proposed that photoperiodism in insects depends on the presence of light-absorbing pigments and that carotenoids and retinoids are one group of possible chromophore for the involved photoreceptors (Veerman and Helle, 1978). However, previous studies revealed that rhythmicity of pupal eclosion was not affected when *Drosophila* was reared on a carotenoid-free medium (Zimmerman and Goldsmith, 1971). In silkworm, researchers performed similar experiments and also observed that carotenoids were dispensable for photoreception and entrainment of the circadian hatching rhythm (Sakamoto et al., 2003; Sakamoto and Shimizu, 1994). Additionally, it has been shown that the photopigment cryptochrome plays a major role in insect photoperiodicity (Collins et al., 2006; Sancar, 2000). Thus, these observations rather contradict a role of carotenoids and NinaB in photoperiodism as related to of egg laying and reproduction.

Thus, one might speculate that our findings in *Bombyx* and *Tribolium* may relate to a role of NinaB in retinoid signaling. In *Drosophila*, NinaB and retinoic acid have been implicated in cellular signaling processes as required for the regeneration of damaged imaginal discs during development (Halme et al., 2010). However, in our opinion, it is unlikely that this process involves canonical retinoid signaling as it occurs in vertebrates (Rhinn and Dolle, 2012). Insect genomes encode an RXR-related protein named Ultraspiracle (USP), but lack retinoic acid receptors (RARs) which act in conjunction with the retinoid X receptor (RXR) in this signal transduction cascade in vertebrates. The vertebrate RXR exclusively binds *cis*-stereoisomers of retinoids (Heyman et al., 1992). Some insect RXR/USP proteins display ligand binding domains with high amino acid sequence identity to their vertebrate RXR counterparts (Hayward et al., 2003). This structural similarity may indicate that some of these transcription factors might use *cis*-retinoids as ligands. As we showed here these *cis*-retinoids can be produced by the enzymatic activity of the NinaB protein. Previous studies showed that RXR/USP is critical for the regulation of vitellogenesis in *Aedes aegypti* and reproduction in *Diploptera punctate* (Hult et al., 2015; Martin et al., 2001). Intriguingly, it has been shown that decreased RXR/USP expression, similar to decreased expression of *ninaB*, inhibited oocyte maturation and completely blocked egg laying in *Tribolium castaneum* (Xu et al., 2010). Thus, we speculate that *cis*-retinoids produced by NinaB can bind at least to *Tribolium* RXR/USP and regulate genes which

are critical for sperm cell development. It remains to be shown which particular retinoid metabolite can bind to RXR/USP and which particular gene activities may depend on this binding. Moreover, the role of the gender dimorphism of the expression of *ninaB* in reproductive organs of different needs to be addressed by further experiments. *BmninaB* was almost exclusively expressed in female reproductive systems of silkworm pupa and moth while *TcninaB* expressed highly in male reproductive systems but not females. Thus, it is yet not clear whether *ninaB* expression in reproductive organs of males and females serves the same or different purposes in different insect species. In future research, the targets of NinaB action need to be identified. Such studies may include analysis of the transcriptome of RNAi treated insects. Furthermore, CRISPR/CAS technology should be applied to establish animals with NinaB mutations and to overcome putative limitations of the RNAi approach.

Taken together, we here showed that NinaB's unique biochemical function is well conserved during insect evolution. The enzyme catalyzed a regio- and stereo-selective conversion of carotenoids into *cis*-retinoids. These *cis*-retinoids are critical for photoreceptor function and maintenance in insects. Additionally, our study of *ninaB* expression profiles and loss-of-function experiments indicate a yet not appreciated role of NinaB in reproduction of some insects. This function might be related to RXR/USP signaling and *cis*-retinoid levels. This observation sheds new light on the evolution of retinoid signaling and warrants further investigation of NinaB function in insect biology in future studies.

Acknowledgements

We thank Dr. Hongbo Jiang from the College of Plant Protection, SWU, for the gift of the beetle strain. We are also grateful to Dr. Zhifeng Xu for technical assistance in injection of beetle dsRNA. This work was supported by National Natural Science Foundation of China (grant numbers 31670123, 31001035), the Fundamental Research Funds for the Central Universities (grant numbers XDJK2016C116, XDJK2017D110, and XDJK2017D111), and Sichuan Academy of Agricultural Sciences Youth Funds (grant number 2018QNJJ-018).

Appendix A. Supplementary data

Supplementary data to this article can be found online at https://doi.org/10.1016/j.ibmb.2019.03.004.

References

Babino, D., Golczak, M., Kiser, P.D., Wyss, A., Palczewski, K., von Lintig, J., 2016. The biochemical basis of vitamin A3 production in arthropod vision. ACS Chem. Biol. 11, 1049–1057.
Borowski, T., Blomberg, M.R., Siegbahn, P.E., 2008. Reaction mechanism of apocarotenoid oxygenase (ACO): a DFT study. Chemistry 14, 2264–2276.
Bybee, S.M., Yuan, F., Ramstetter, M.D., Llorente-Bousquets, J., Reed, R.D., Osorio, D., Briscoe, A.D., 2012. UV photoreceptors and UV-yellow wing pigments in Heliconius butterflies allow a color signal to serve both mimicry and intraspecific communication. Am. Nat. 179, 38–51.
Collins, B., Mazzoni, E.O., Stanewsky, R., Blau, J., 2006. Drosophila CRYPTOCHROME is a circadian transcriptional repressor. Curr. Biol. 16, 441–449.
Demmig-Adams, B., Adams 3rd, W.W., 2002. Antioxidants in photosynthesis and human nutrition. Science 298, 2149–2153.
Feltwell, J., Valadon, L.R., 1970. Plant Pigments identified in the common blue butterfly. Nature 225, 969.
Grayson, J.O.Y., Edmunds, M., Hilary Evans, E., Britton, G., 2008. Carotenoids and colouration of poplar hawkmoth caterpillars (Laothoe populi). Biol. J. Linn. Soc. Lond. 42, 457–465.
Haliscak, J.P., Beeman, R.W., 1983. Status of malathion resistance in five genera of beetles infesting farm-stored corn, wheat, and oats in the United States. J. Econ. Entomol. 76, 717–722.
Halme, A., Cheng, M., Hariharan, I.K., 2010. Retinoids regulate a developmental checkpoint for tissue regeneration in Drosophila. Curr. Biol. 20, 458–463.
Harris, W.A., Ready, D.F., Lipson, E.D., Hudspeth, A.J., Stark, W.S., 1977. Vitamin A deprivation and Drosophila photopigments. Nature 266, 648–650.
Hayward, D.C., Dhadialla, T.S., Zhou, S., Kuiper, M.J., Ball, E.E., Wyatt, G.R., Walker, V.K., 2003. Ligand specificity and developmental expression of RXR and ecdysone receptor in the migratory locust. J. Insect Physiol. 49, 1135–1144.
Heyman, R.A., Mangelsdorf, D.J., Dyck, J.A., Stein, R.B., Eichele, G., Evans, R.M., Thaller, C., 1992. 9-cis retinoic acid is a high affinity ligand for the retinoid X receptor. Cell 68, 397–406.
Hult, E.F., Huang, J., Marchal, E., Lam, J., Tobe, S.S., 2015. RXR/USP and EcR are critical for the regulation of reproduction and the control of JH biosynthesis in Diploptera punctata. J. Insect Physiol. 80, 48–60.
Isono, K., Tanimura, T., Oda, Y., Tsukahara, Y., 1988. Dependency on light and vitamin A derivatives of the biogenesis of 3-hydroxyretinal and visual pigment in the compound eyes of Drosophila melanogaster. J. Gen. Physiol. 92, 587–600.
Kiefer, C., Sumser, E., Wernet, M.F., Von Lintig, J., 2002. A class B scavenger receptor mediates the cellular uptake of carotenoids in Drosophila. Proc. Natl. Acad. Sci. U. S. A 99, 10581–10586.
Krinsky, N.I., 1993. Actions of carotenoids in biological systems. Annu. Rev. Nutr. 13, 561–587.
Krinsky, N.I., Landrum, J.T., Bone, R.A., 2003. Biologic mechanisms of the protective role of lutein and zeaxanthin in the eye. Annu. Rev. Nutr. 23, 171–201.
Mallet, J., Joron, M., 1999. Evolution of diversity in warning color and mimicry: polymorphisms, shifting balance, and speciation. Annu. Rev. Ecol. Syst. 30, 201–233.
Martin, D., Wang, S.F., Raikhel, A.S., 2001. The vitellogenin gene of the mosquito Aedes aegypti is a direct target of ecdysteroid receptor. Mol. Cell. Endocrinol. 173, 75–86.
Oberhauser, V., Voolstra, O., Bangert, A., von Lintig, J., Vogt, K., 2008. NinaB combines carotenoid oxygenase and retinoid isomerase activity in a single polypeptide. Proc. Natl. Acad. Sci. U. S. A 105, 19000–19005.
Parthasarathy, R., Tan, A., Sun, Z., Chen, Z., Rankin, M., Palli, S.R., 2009. Juvenile hormone regulation of male accessory gland activity in the red flour beetle. Tribolium castaneum. Mech. Dev. 126, 563–579.
Rhinn, M., Dolle, P., 2012. Retinoic acid signalling during development. Development 139, 843–858.
Rothschild, M., Mummery, R., Farrell, C., 1986. Carotenoids of butterfly models and their mimics (Lep: papilionidae and Nymphalidae). Biol. J. Linn. Soc. Lond. 28, 359–372.
Sakamoto, K., Asai, R., Okada, A., Shimizu, I., 2003. Effect of carotenoid depletion on the hatching rhythm of the silkworm, *Bombyx mori*. Biol. Rhythm Res. 34, 61–71.
Sakamoto, K., Shimizu, I., 1994. Photosensitivity in the circadian hatching rhythm of the carotenoid-depleted silkworm, *Bombyx mori*. J. Biol. Rhythm. 9, 61–70.
Sakudoh, T., Iizuka, T., Narukawa, J., Sezutsu, H., Kobayashi, I., Kuwazaki, S., Banno, Y., Kitamura, A., Sugiyama, H., Takada, N., Fujimoto, H., Kadono-Okuda, K., Mita, K., Tamura, T., Yamamoto, K., Tsuchida, K., 2010. A CD36-related transmembrane protein is coordinated with an intracellular lipid-binding protein in selective carotenoid transport for cocoon coloration. J. Biol. Chem. 285, 7739–7751.
Sakudoh, T., Kuwazaki, S., Iizuka, T., Narukawa, J., Yamamoto, K., Uchino, K., Sezutsu, H., Banno, Y., Tsuchida, K., 2013. CD36 homolog divergence is responsible for the selectivity of carotenoid species migration to the silk gland of the silkworm *Bombyx mori*. J. Lipid Res. 54, 482–495.
Sakudoh, T., Sezutsu, H., Nakashima, T., Kobayashi, I., Fujimoto, H., Uchino, K., Banno, Y., Iwano, H., Maekawa, H., Tamura, T., Kataoka, H., Tsuchida, K., 2007. Carotenoid silk coloration is controlled by a carotenoid-binding protein, a product of the Yellow blood gene. Proc. Natl. Acad. Sci. U. S. A 104, 8941–8946.
Sancar, A., 2000. Cryptochrome: the second photoactive pigment in the eye and its role in circadian photoreception. Annu. Rev. Biochem. 69, 31–67.
Seki, T., Vogt, K., 1998. Evolutionary aspects of the diversity of visual pigment chromophores in the class insecta. Comp. Biochem. Physiol. B Biochem. Mol. Biol. 119, 53–64.
Sui, X., Kiser, P.D., Lintig, J., Palczewski, K., 2013. Structural basis of carotenoid cleavage: from bacteria to mammals. Arch. Biochem. Biophys. 539, 203–213.
Toews, D.P.L., Hofmeister, N.R., Taylor, S.A., 2017. The evolution and genetics of carotenoid processing in animals. Trends Genet. 33, 171–182.
Tsuchida, K., Sakudoh, T., 2015. Recent progress in molecular genetic studies on the carotenoid transport system using cocoon-color mutants of the silkworm. Arch. Biochem. Biophys. 572, 151–157.
Veerman, A., Helle, W., 1978. Evidence for the functional involvement of carotenoids in the photoperiodic reaction of spider mites. Nature 275, 234.
von Lintig, J., 2010. Colors with functions: elucidating the biochemical and molecular basis of carotenoid metabolism. Annu. Rev. Nutr. 30, 35–56.
von Lintig, J., 2012. Provitamin A metabolism and functions in mammalian biology. Am. J. Clin. Nutr. 96, 1234S–1244S.
von Lintig, J., Dreher, A., Kiefer, C., Wernet, M.F., Vogt, K., 2001. Analysis of the blind Drosophila mutant ninaB identifies the gene encoding the key enzyme for vitamin A formation in vivo. Proc. Natl. Acad. Sci. U. S. A 98, 1130–1135.
von Lintig, J., Vogt, K., 2000. Filling the gap in vitamin A research. Molecular identification of an enzyme cleaving beta-carotene to retinal. J. Biol. Chem. 275, 11915–11920.
Voolstra, O., Oberhauser, V., Sumser, E., Meyer, N.E., Maguire, M.E., Huber, A., von Lintig, J., 2010. NinaB is essential for Drosophila vision but induces retinal degeneration in opsin-deficient photoreceptors. J. Biol. Chem. 285, 2130–2139.
Wang, T., Jiao, Y., Montell, C., 2007. Dissection of the pathway required for generation of vitamin A and for Drosophila phototransduction. J. Cell Biol. 177, 305–316.
Weiszmann, R., Hammonds, A.S., Celniker, S.E., 2009. Determination of gene expression patterns using high-throughput RNA in situ hybridization to whole-mount Drosophila embryos. Nat. Protoc. 4, 605–618.
Xu, J., Tan, A., Palli, S.R., 2010. The function of nuclear receptors in regulation of female reproduction and embryogenesis in the red flour beetle, Tribolium castaneum. J. Insect Physiol. 56, 1471–1480.
Yang, J., O'Tousa, J.E., 2007. Cellular sites of Drosophila NinaB and NinaD activity in vitamin A metabolism. Mol. Cell. Neurosci. 35, 49–56.
Zimmerman, W.F., Goldsmith, T.H., 1971. Photosensitivity of the circadian rhythm and of visual receptors in carotenoid-depleted Drosophila. Science 171, 1167–1169.
Ziouzenkova, O., Plutzky, J., 2008. Retinoid metabolism and nuclear receptor responses: new insights into coordinated regulation of the PPAR-RXR complex. FEBS Lett. 582, 32–38.